

REVIEW Neuro/Head and Neck Radiology

Post-treatment Magnetic Resonance Imaging assessment of brain gliomas

Despoina Voultsinou, Triantafillos Gerukis
Radiology Department, "G. Papanikolaou" Hospital, Thessaloniki, Greece

SUBMISSION: 7/8/2020 | ACCEPTANCE: 28/10/2020

ABSTRACT

Imaging is essential in brain glioma diagnosis, treatment and follow up. Diversity in genetic and phenotypic architectures of brain glioma makes imaging evaluation challenging. Glioma appearance on follow up examination correlates with the response to therapeutic scheme and therapy side effect. Standard magnetic resonance (MR) imaging and advanced techniques (diffusion, perfusion, spectroscopy) are crucial in evaluation of post-treatment response of brain gliomas. The *Response Assessment in Neu-*

ro Oncology criteria evolved as an objective guide for imaging assessment of response to treatment in brain gliomas. This article presents MR imaging of brain gliomas response to therapy (complete, partial response, stable disease, progress or recurrence) and the side-effects of the various therapeutic schemes (surgery, radiation, chemotherapy, antiangiogenic therapy, immunotherapy induced toxicity). Pseudoprogression and pseudoresponse are also discussed.



KEY WORDS

Central nervous system; Magnetic resonance imaging; Brain neoplasms; Perfusion imaging; Diffusion weighted imaging



CORRESPONDING AUTHOR, GUARANTOR

Corresponding author: Despoina Voultsinou, Radiology Department, "G. Papanikolaou" Hospital, Papanikolaou Ave, 57010, Thessaloniki, Greece, Email: divou2@yahoo.gr
Guarantor: Triantafillos Gerukis, Radiology Department, "G. Papanikolaou" Hospital, Papanikolaou Ave, 57010, Thessaloniki, Greece, Email: gerukis@yahoo.gr

1. Introduction

The incidence rate of brain gliomas is about 5 per 100,000 person-years. It constitutes 2% of all adult cancers [1-7]. According to the World Health Organisation (WHO), gliomas are categorised as grades I-IV, on the basis of their histological appearance [7, 8]. The most aggressive form, particularly in adults, is that of glioblastoma multiforme (GBM), with the diffuse type being by far the more frequent [1-8]. Malignant gliomas correlate with 80% of all malignant brain tumours [1-8]. Brain tumour heterogeneity is related to the variability of genetic, metabolic and microenvironment composition of brain tumour cells. A new concept for brain glioma classification and treatment has been derived from genomic profiling [8-10]. According to the status of the catalyst isocitrate dehydrogenase (IDH) [10], diffusely infiltrating gliomas are classified into three separate groups, each group with its specific natural history, response to treatment and outcome. IDH mutant 1p/19q co-deleted tumours develop better prognosis and are most often associated with oligodendroglial tumours; IDH-mutant, 1p/19q non-co-deleted tumours have intermediate outcome and are most often associated with astrocytic histological type and IDH wild-type, develop mostly poor prognosis and are associated with high-grade (III or IV) tumours [8-10].

Brain gliomas treatment is individualised, according to the location of brain lesion, histologic grade, genotype, patient clinical status and resectability, in order to improve prognosis and side effects limitation [11-13]. For IDH [10-13], wild-type (high grade gliomas), therapy is directed to local safe resection with minimal induced deficit. For diffuse astrocytomas, oligodendrogliomas and low grade gliomas the use of intraoperative navigation, fusion, digital tractography, cortical mapping, and intraoperative neuromonitoring constitute a great aid [14-21]. Radiation and chemotherapy (temozolomide-alkylating agent) according to the Stupp protocol (also known as chemoradiation), are applied when necessary and improve survival significantly [22-26]. Antiangiogenic agents such as bevacizumab, an antibody against vascular endothelial growth factor (VEGF), are considered second-line agents with poor survival benefit that is usually reserved for recurrent disease. Re-

section with clear margins is not possible for diffuse astrocytomas and oligodendrogliomas due to their highly infiltrative nature. Newer therapies, such as immunotherapy [27-29], nanotechniques, hyperthermia, receptor mediated transport, cell-penetrating peptides and cell mediated delivery demonstrate promising results. Low grade gliomas are also not so well curable, although they bear a more indolent clinical course, frequently exhibiting gliomagenesis to high-grade glioma in a high percentage of patients. The individualised therapeutic scheme (time, extent of surgery, radiation therapy, chemotherapy) is balanced between survival benefits and treatment-related side effects.

Despite advanced treatment techniques and protocols, the median survival rate of brain tumours is still poor [6]. High-grade gliomas (HGG) have a survival rate of only 2 years for 26.5% whereas low-grade gliomas (LGG) have a 5-year survival of 58-72% [1-6].

2a. Normal postoperative status

During craniotomy the bone flap is replaced at the end of the procedure. According to its location, the flap is named as frontal, bifrontal etc. Skin closure is performed with metallic scalp clips, that produce artefacts on CT and MR images. In the early postoperative period, scalp swelling is common. It is formed from a mixture of oedematous fluid, haemorrhage, cerebro-spinal fluid (CSF) and air. Swelling typically resolves over several weeks [30-32]. The margins of bone flaps initially are well defined, straight-edged with "tram-track" discontinuities. With time, they become more rounded.

At postoperative imaging, it can be difficult to determine the precise location of fluid collections (blood, CSF and air), but they are more often extradural than subdural [30-32]. Extradural fluid collections immediately beneath the bone flap are to be expected after craniotomy. Small amounts of haematoma in the scalp can be seen as thin (1-3 mm thick) extradural collections. The intraoperative use of haemostatic agents, such as oxidised regenerated cellulose, can accelerate the formation of methaemoglobin, which produces areas of hyperintensity on T1- and T2-weighted images earlier than expected. The normal dura mater appears as a thin hypointense layer

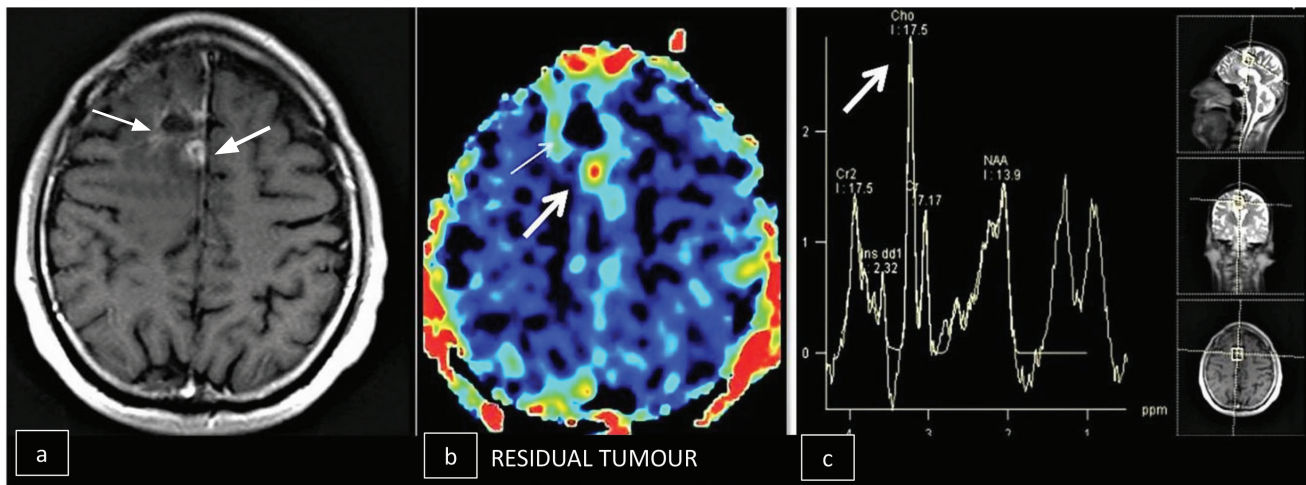


Fig. 1. A 45-year-old male with residual tumour, three days after operation for anaplastic astrocytoma. **a)** Axial contrast enhanced T1-w MR image demonstrates the postoperative cavity with an expected minimal peripheral enhancement (thin arrow) and adjacent increased nodular enhancement (thick arrow), **b)** rCBV map shows decreased rCBV values of the wall of the postoperative cavity (thin arrow) and increased values at the center of the enhancing nodule (thick arrow), **c)** MRS with long TE, at the center of the enhancing and increased rCBV value-nodule, illustrates increased levels of choline peaks at the position 3.2 p.m.

on both T1- and T2-weighted MR images compared to gray matter.

After craniotomy, normal postoperative contrast enhancement (**Fig. 1**) on MR imaging is seen earlier and lasts longer than on CT. Between the margins of the bone flap and the calvaria, neovascular granulation tissue forms and may enhance within the first year after surgery. The dura mater after surgery enhances in a smooth linear pattern as early as 9 hours and can last as long as 40 years [30-32]. The surgical margins of brain parenchyma may begin to enhance within 17 hours. Initially they appear as thin linear areas of enhancement in some patients. This enhancement increases with time. In the 6th postoperative day, the enhancement pattern becomes thicker and nodular and is seen in all patients. It usually resolves within 1 month after surgery [30-32]. Some amount of intracranial air, most often in the subdural space over the frontal lobe, should be expected on early postoperative imaging. In a retrospective analysis of CT findings in patients who underwent supratentorial craniotomy, pneumocephalus was present in 100% of patients 2 days after surgery, in 75% of patients 7 days after surgery, in 59.6% of patients in the 2nd postoperative week, and in 26.3% of patients in the 3rd postoperative week. No pneumocephalus

was found after 3 weeks [30-32].

2b. Postoperative complications-any deviation from normal postoperative status

The most common post-surgical complication is iatrogenic stroke with an incidence of 1.6%. Iatrogenic ischaemic stroke is related to the proximity of the brain tumour to the central perforating arteries. It carries a nine-fold increased risk of hospital mortality [30-32]. The second most common post-surgical complication is intracranial haemorrhage with an incidence of 1.0% (1.1% of patients require surgical evacuation).

A less common or rare complication is post-surgical infection. It typically develops in patients with a depressed immune status. It can manifest as bone flap infection (44%), subdural empyema, cerebritis, abscess and meningitis (incidence of approximately 0.1%). Early recognition is extremely important in order to restrict morbidity and mortality. Bone flap infection develops 1-2 weeks after surgery but may not manifest for months. Diffusion-weighted imaging is less sensitive in depicting infection in post-operative patients, especially in extradural location [32], with false-negative rates of 47% for extradural abscesses and 29% for subdural empyema. Thus, the absence of

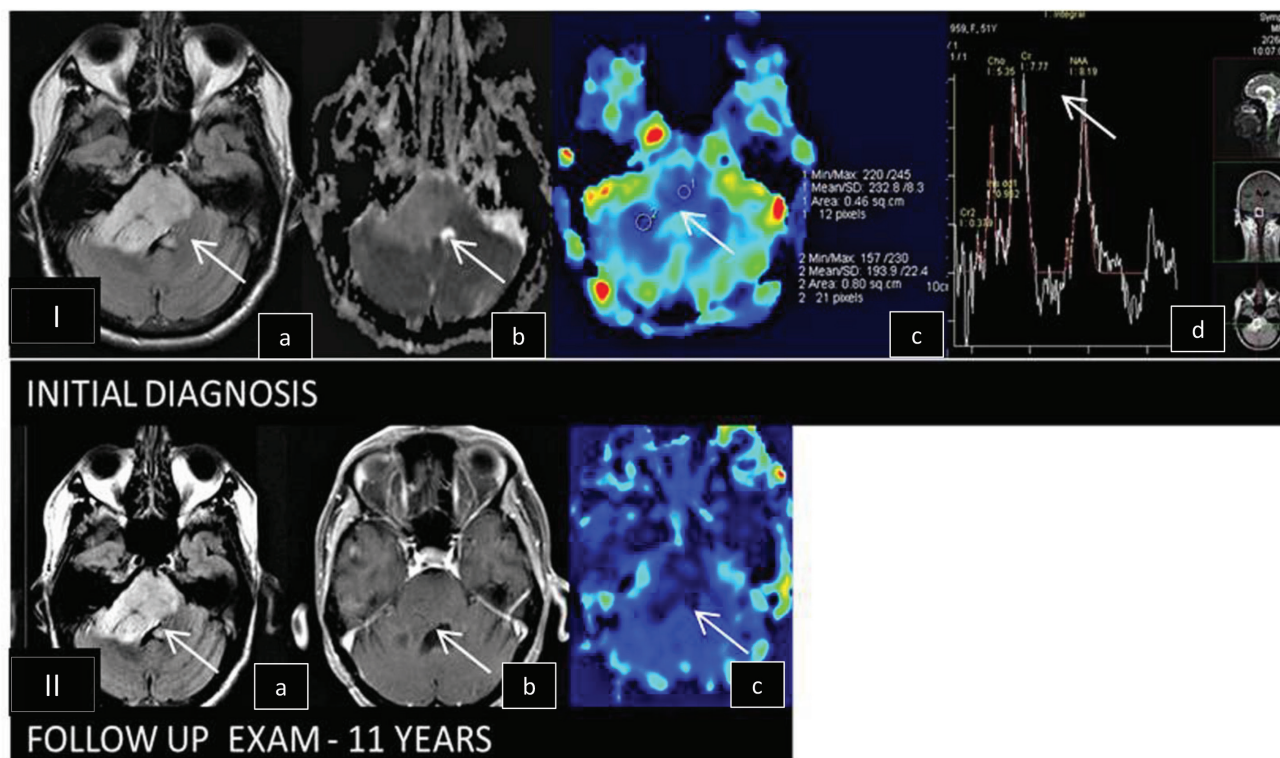


Fig. 2. Follow up in a 51-year-old female with a stable fibrillary low grade astrocytoma diagnosed by stereotactic biopsy, 11 years ago. **I.** Axial MRI, at the time of the initial diagnosis: **a)** FLAIR shows a diffuse area of increased signal intensity of the brain stem and right cerebellar peduncle (arrow) with **b)** ADC map shows, increased ADC values (arrow), **c)** rCBV map, rCBV values are within normal limits (arrow) and **d)** short TE MRS shows increased values for the metabolite myo-inositol at 0.962 (arrow). **II.** Follow up examination -11 years after the initial diagnosis **a)** FLAIR shows unchanged findings (arrow), **b)** axial contrast-enhanced T1-w MR image shows no contrast enhancement and **c)** rCBV map shows normal CBV values.

restricted diffusion within a postoperative fluid collection does not reliably exclude the possibility of infection [31, 32].

Tension pneumocephalus is a neurosurgical emergency. CT appearances include the “peaking” sign (subdural air collections compress the frontal lobes) and the “Mount Fuji” sign (widening of the inter-hemispheric space from compression and separation of the frontal lobes). Diagnosis should only be made with clinical correlation, since similar findings may be seen in asymptomatic patients.

3. Post-treatment response of brain gliomas

Different criteria were used to assess treatment response of high grade gliomas, such as perilesional mass effect and tumour size, since 1977. The first objective criteria (Macdonald criteria) for radio-

logic evaluation of high-grade gliomas response to treatment were published in 1990 [33]. Tumour enhancement on CT was evaluated in accordance with decreased need for steroids and stable or improved clinical status. Contrast medium enhancement is sensitive but not a specific marker of tumour regression and may represent post-therapy changes. MR imaging [34-45], in addition to morphological characteristics (size, necrosis, oedema), offers crucial information on the non-enhancing part of the tumour (T2-w/FLAIR) and has become the standard neuroimaging technique used to assess treatment response. The Response Assessment in Neuro-Oncology (RANO) criteria released new standardised response criteria for clinical trials in brain tumours in 2010. This RANO system offers detailed and reproducible evaluation brain tumour response to therapy. Although other

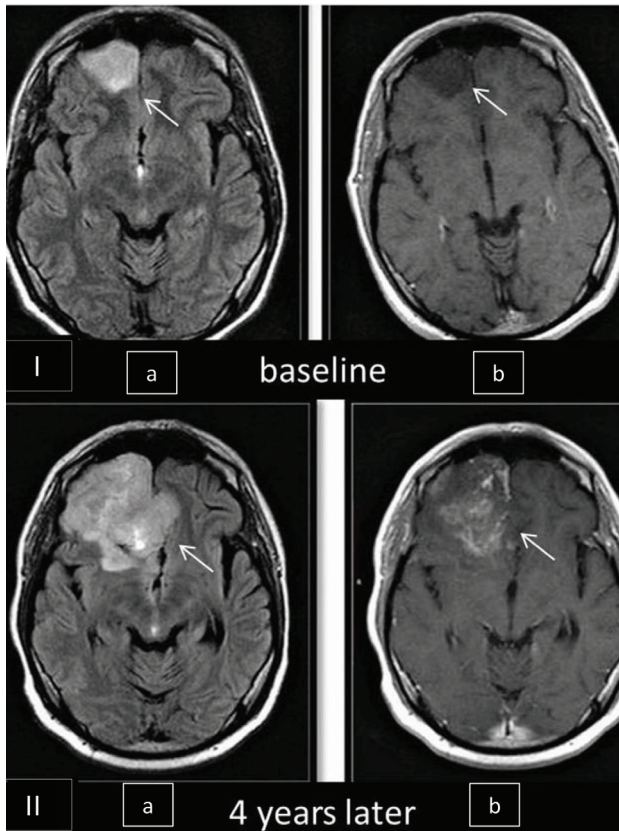


Fig. 3. Follow up of a low-grade astrocytoma-Gliomagenesis. **I.** Baseline axial MR images, of a low grade astrocytoma, at the time of the diagnosis **a)** FLAIR sequence shows abnormal signal intensity at the right frontal lobe, **b)** post-gadolinium T1-w image shows no contrast enhancement. **II.** Progression to high grade (IV) astrocytoma, on follow up examination 4 years later, **a)** FLAIR sequence shows significant increment of abnormal signal at the right frontal lobe with more heterogeneous appearance (arrow) and **b)** post-gadolinium T1-w image demonstrates inhomogeneous contrast enhancement (arrow).

criteria have been published over the last years, the RANO criteria are currently the most widely used in clinical practice [34-45].

3a. Practical points

Practical points on measurements

Brain lesions can be solitary or multiple, measurable or non measurable. A measurable lesion is one with sharp, well defined margins, with two perpendicular diameters of at least 10 mm, visible on more than 2 axial slices, hyperintense on T2/FLAIR images, showing contrast-enhancement. A non-measurable lesion

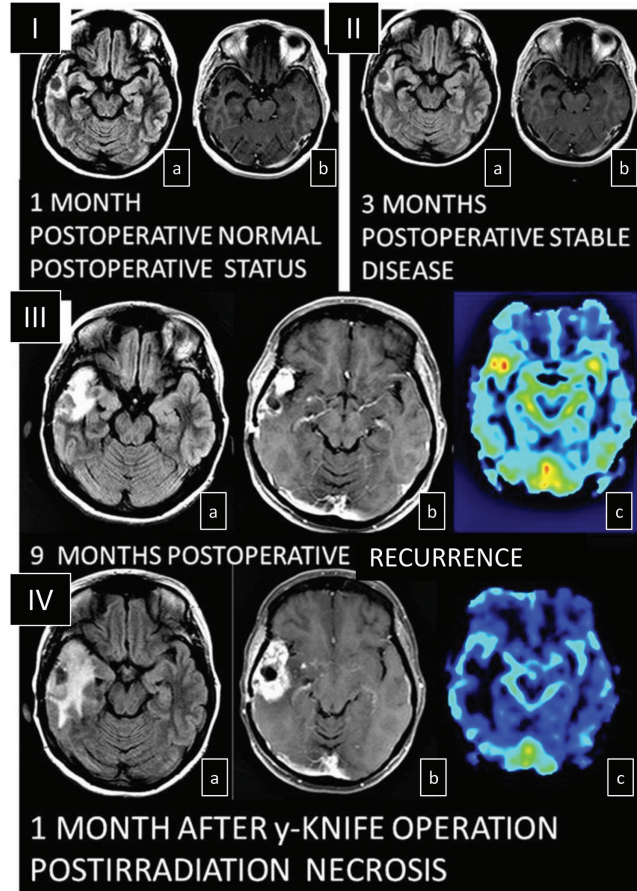


Fig. 4. Serial follow up examinations of a patient with anaplastic astrocytoma at 1st, 3rd, 9th postoperative month and 1st month after γ -knife operation. **I.** Normal postoperative status: 1 month post operative, a cavity is seen **a)** FLAIR shows minimal brain oedema, **b)** contrast-enhanced T1-w image showing postoperative meningeal enhancement, **II.** Stable disease, 3 months post operative, with unchanged findings both on FLAIR (**a**) and contrast-enhanced T1-w (**b**) images. **III.** Recurrence, 9 months post operative, **a)** FLAIR, shows moderate brain oedema, **b)** contrast-enhanced T1-w image shows enhancement and **c)** CBV map shows high rCBV values, **IV.** Irradiation necrosis, 1 month after γ -knife treatment, **a)** FLAIR shows increase of the extent of brain oedema, **b)** contrast-enhanced T1-w image shows increase of the extent of enhancement and **c)** PWI shows normal rCBV value.

is a contrast enhancing lesion with either unidimensionally measurable lesion or with maximal perpendicular diameters of less than 10 mm, with ill-defined margins. Non-measurable brain lesions usually represent the most common imaging feature of lower-grade tumours. In the case of multiple lesions, the

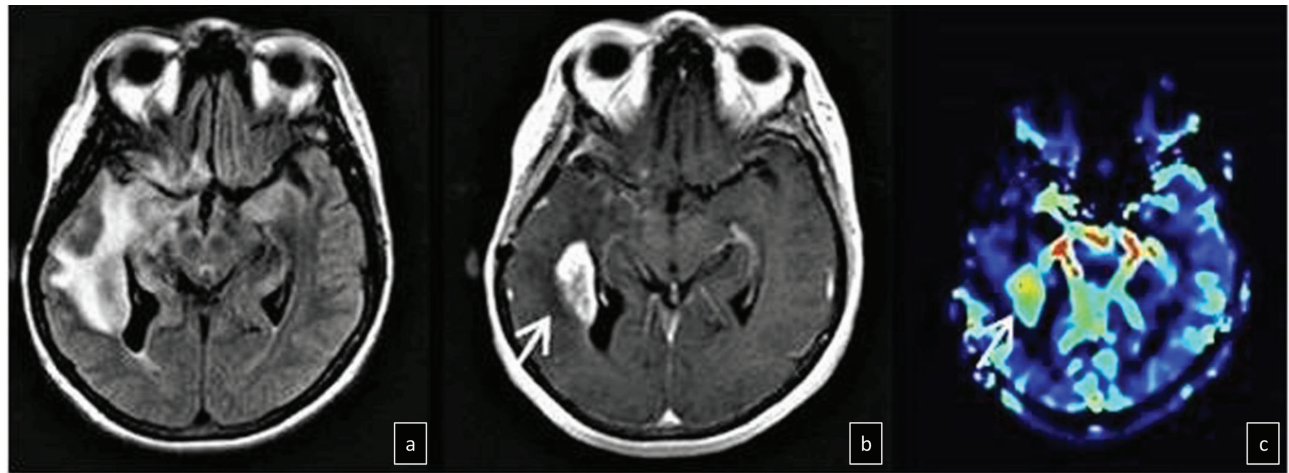


Fig. 5. Recurrence in a male patient who was operated and irradiated for anaplastic astrocytoma, one year prior to current MR imaging. Axial views **a**) FLAIR images show diffuse brain oedema of the right temporo-parietal lobe, **b**) contrast-enhanced T1-w image shows intense enhancement (arrow) and **c**) increased rCBV values are shown at the corresponding maps at the area of maximal contrast medium enhancement (arrow).

largest lesions are preferably measured, but emphasis should also be placed on lesions that allow reproducible measurements.

Practical points on timing

It is important to perform MR imaging at follow examinations within specific time periods, according to the RANO criteria.

- The first follow up examination is suggested to take place within 3 days post operatively to assess the extension of any residual lesion (**Fig. 1**). Contrast enhancement in the margins of the postoperative cavity corresponds at that period of time to residual tumour (“diagnostic window”). Diffusion-weighted imaging shows the cytotoxic oedema, a normal postoperative complication. Analogous to ischaemic stroke, most of those areas of restricted diffusion finally enhance after 48 hours and are attributed to the presence of granulation tissue.

- Post-treatment follow up includes MR examination every 6 months for low grade gliomas (**Figs. 2, 3**) and every 3 month intervals for high grade gliomas (**Figs. 4, 5**) to evaluate any tumour recurrence.

- An MR examination should include T2-w, FLAIR and T1-w sequences with and without contrast medium administration in three planes, T2 Gradient Echo when it is needed, as well as advanced MR imaging, including diffusion weighted imaging (DWI), perfusion weighted

imaging (PWI) and spectroscopy, when needed.

- Ideally the examinations should match each other as closely as possible; same technique of examination should be used. Proper use of contrast is especially important (dose, concentration and optimal delay time).

3b. Post-treatment response criteria

Brain tumour imaging techniques, both conventional and advanced MR imaging (DWI, PWI, and spectroscopy) focus on a new appearing or a pre-existing lesion and examine both the enhancing part and the non-enhancing T2/FLAIR component.

Brain tumour post-treatment assessment is based on imaging and clinical criteria (clinical status and corticosteroid use). Accordingly, treatment response is classified into 4 categories [33-45]. The results are compared to the baseline scan. Complete response is associated with a disappearance of the enhancing part, stable or improved non-enhancing (T2/FLAIR) part, and no lesion for at least 4 weeks on imaging. The patients must be off corticosteroids (or on physiologic replacement doses only) and stable or improved clinically. In partial response, there is greater than 50% decrease in the total diameters of the measurable enhancing lesions, improved non-enhancing (T2/FLAIR) part, and no new lesion on imaging for at least 4 weeks. The patient must be at the same

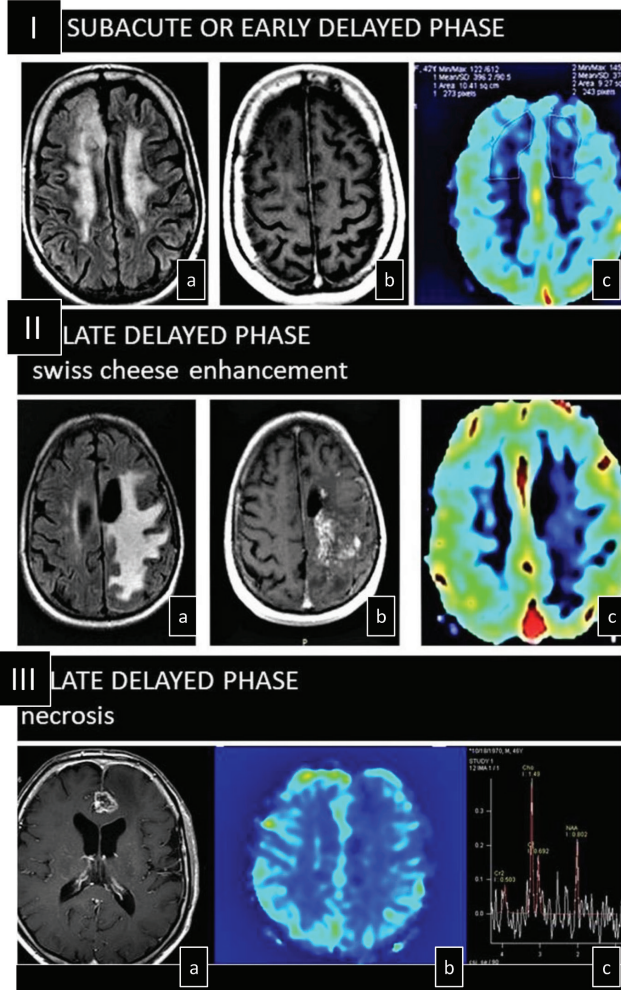


Fig. 6. Spectrum of radiation effect on brain parenchyma in three different patients. **I.** Early delayed phase MR imaging in a 72-year-old female with irradiated low grade astrocytoma 7 years ago. **a)** FLAIR sequence shows bilateral periventricular brain oedema, **b)** post-gadolinium T1-w showing no contrast enhancement and **c)** normal rCBV values at corresponding maps. **II.** Late delayed phase in a 65-year-old male with post-irradiation leukoencephalopathy operated for anaplastic astrocytoma 1 year after irradiation. Late delayed phase **a)** FLAIR sequence shows unilateral periventricular brain oedema, **b)** post-gadolinium scan shows swiss cheese enhancement, **c)** normal rCBV values at corresponding maps. **III.** Late delayed phase in a 56-year-old male with post-irradiation necrosis, who was operated for brain glioma 1 year ago and underwent chemoradiation scheme. Late delayed phase, **a)** post gadolinium scan shows peripheral contrast medium enhancement, with **b)** normal rCBV values at the corresponding map and **c)** MRS-increased choline levels.

or lower dose of corticosteroids, stable or improved clinically. Stable disease (Figs. 2, 4) correlates with stable imaging results, with the patient at the same or lower dose of corticosteroids, stable or improved clinically.

Progressive disease may comprise any of the following (Fig. 3):

- greater than 25% increase in the total diameters of enhancing parts compared to baseline scan (if no decrease) or best response on stable or increasing dose corticosteroids;
- significant increase in T2/FLAIR non-enhancing lesion on stable or increasing doses of corticosteroids compared to baseline scan or best response after initiation of therapy not caused by comorbid events (e.g. radiation therapy, demyelination, ischaemic injury, infection, seizures, postoperative changes or other treatment effects);
- progression of non-measurable lesions;
- any new lesion;
- clear clinical deterioration not attributable to other causes apart from the tumour (e.g. seizures, medication adverse effects, complications of therapy, cerebrovascular events, infection etc) or changes in corticosteroid dose.

Low grade gliomas in post-treatment assessment may demonstrate residual lesion, post irradiation necrosis or progression in a similar manner with high grade gliomas. Typical findings for progressive lower-grade glioma are increasing non-enhancing lesions on T2-w or FLAIR and development of contrast enhancement, decreased ADC values or increase in rCBV values, indicating malignant transformation-gliomagenesis. Increment in rCBV values may precede by 12 months the development of contrast medium enhancement, because it is not associated with dysfunction or breakdown of blood brain barrier.

Assessment with MR imaging is not without pitfalls [34-45]. New contrast-enhancing lesions are not always indicative of tumour recurrence. Non-tumoural increase (pseudoprogression, radiation necrosis) and decrease (pseudoresponse) in enhancement have been observed [46-50]. It is well-established that the T2/FLAIR hyperintensity surrounding an enhancing tumour comprises not only vasogenic oedema but also neoplastic infiltration. After surgery, radiation

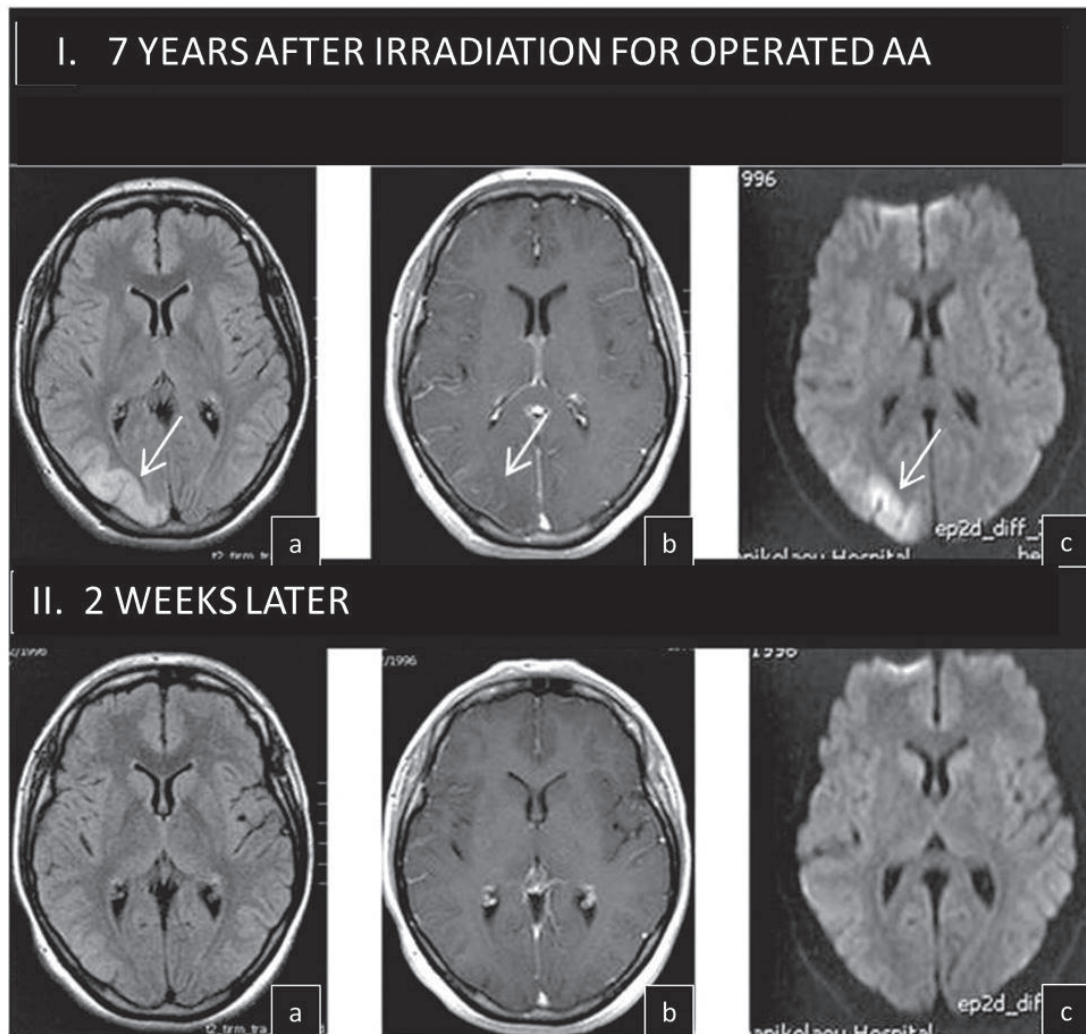


Fig. 7. Smart syndrome. **I.** Patient operated and irradiated for anaplastic astrocytoma seven years ago. **a)** FLAIR sequence illustrates cortical swelling of the right occipital lobe with a gyriform hyperintensity (arrow), **b)** Contrast-enhanced T1-w image shows no enhancement (arrow) and **c)** DWI shows restricted diffusion (arrow). **II.** 2 weeks later a self-limited response is seen, **a)** FLAIR sequence **b)** post-gadolinium scan **c)** and DWI b value -1000, with normal findings. The patient passed away.

therapy and temozolomide, therapy-related inflammatory changes also present as T2/FLAIR hyperintensity. Neoplastic infiltration is associated with loss of gray-white matter differentiation and increased mass effect. On the other hand, inflammatory and therapy related changes typically spare the brain cortex. T2-w images are recommended for more accurate evaluation of blurring of the grey-white junction, findings that may be subtle on FLAIR.

4. Tumour recurrence

Due to the absence of objective criteria, the diagnosis

of tumour recurrence may be challenging (Figs. 4c, 5, 6), even through histopathologic analysis. Recent reports showed only minimal reproducibility in the final diagnosis of active tumour and treatment effect [51-56].

5. Therapy consequences on post-treatment response

5a. Radiation therapy

According to current guidelines recommendation, radiation therapy is focused on the surgical cavity and a 20 mm margin that corresponds to the most

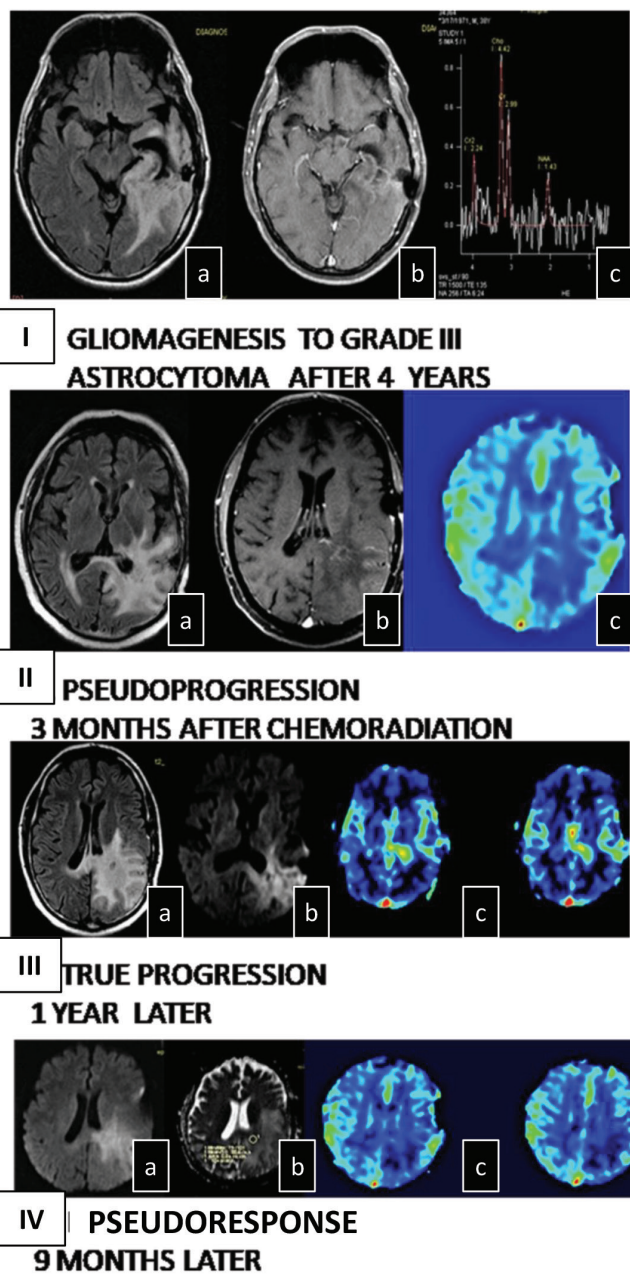


Fig 8. A 62-year-old female patient, who was operated for grade II astrocytoma and underwent chemoradiation scheme. **I.** Gliomagenesis: transformation of grade II to grade III astrocytoma, 4 years after the initial diagnosis **a)** FLAIR sequence shows diffuse brain oedema in the left parieto occipital lobe; **b)** post-gadolinium T1-w shows no enhancement; **c)** MRS shows increased peak of choline. **II.** Pseudoprogession: 3 months after chemoradiation **a)** FLAIR sequence shows increasing brain oedema; **b)** post-gadolinium T1-w image shows increased enhancement with **c)** low rCBV values. **III.** True progression: Follow examination 1 year later **a)** FLAIR sequence shows further extension of brain oedema with **b)** DWI b- value 1000 restricted diffusion and **c)** increased rCBV values. **IV.** Pseudo-response: 9 months after bevacizumab therapy **a)** DWI b- value 1000 shows restricted diffusion, **b)** ADC map decreased ADC values and **c)** decreased rCBV, at rCBV maps. The patient passed away.

frequent site of recurrence. For accurate planning, a pre-operative brain CT scan is performed and fused with a post-operative MR imaging. The pre-operative CT scan also provides information about the isodose curves (lines with the same percentage of radiation dose). A graph is plotted with the radiation dose that is received in each brain region.

Radiation therapy induced brain parenchyma injury may involve brain vessels, myelin sheaths and neuronal cells [57, 58]. Radiation induced injury is related to the radiation dose and the time elapsed since radiation exposure. The injuries induced by radiation are classified as acute, subacute or chronic [57, 58]. Acute phase changes are attributed to endothelial injury that develops from the first days to several weeks after irradiation exposure. Changes are initially related to vascular permeability that results in brain oedema and subsequently with vascular damage. Patients typically present signs of brain oedema (headache and drowsiness). Conventional and advanced MR imaging does not show any specific findings, it may be normal or show brain oedema in both hemispheres with spontaneous resolution on follow up examinations.

Subacute or early delayed phase (**Fig. 6 I, II**) changes are attributed in addition to vascular damage to demyelination due to decreased oxygen supply. They develop one to six months after therapy. Patients typically present signs of brain oedema and attention or memory deficit. MR imaging may demonstrate brain oedema or non-specific signal intensity changes of the white matter, basal ganglia or cerebral pedicles with spontaneous resolution. Advanced MR imaging does not seem to offer any specific finding.

In the late delayed phase (**Fig. 6 I, II**) the changes are attributed to a more serious injury; in addition to vascular injury and demyelination, glial cell involvement also occurs. Usually it is observed 3-12 months from the initiation of radiotherapy, although it can develop many years or decades later. The damage is irreversible. Conventional MR imaging can demonstrate diffuse leukoencephalopathy or focal postirradiation necrosis (PIN). Post irradiation leukoencephalopathy is most often located periventricularly or subcortically. It may not exhibit any contrast enhancement. Focal PIN constitutes the more serious complication of the spectrum of post-

irradiation injuries. It is seen in about 5-24% of irradiated patients with higher incidence in patients on chemoradiation and has a tremendous impact on patient quality of life [52-58]. PIN is worsening with time. Discrimination between normal ageing and vasculopathy is difficult.

In conventional MR imaging, PIN presents with varying MR patterns [52-58]. Most frequently PIN is visualised as a cystic white matter or cortical (deep cortex only) lesion in the irradiated area. Microhaemorrhages may coexist. Usually the deviation of midline structures is minimal or is not seen. Typical imaging patterns on contrast-enhanced images are those of “soap bubbles appearance”, “Swiss cheese” (Fig. 6 II) or islands of contrast enhancement, although nodular or peripheral enhancement (Fig. 4 IV) may be detected.

Radiation therapy versus recurrent neoplasm

A serious diagnostic dilemma is the discrimination between recurrent neoplasm and radiation changes, especially PIN [52-56]. These two entities overlap considerably, even on histopathology analysis. At follow up examination both lesions may remain unchanged or show an increase in size. Differences in the degree of contrast enhancement between recurrence (increased value, 5.85%) and irradiation necrosis (low value, 1.9%), may contribute in the differential diagnosis. Conventional MR imaging may be inadequate for reliably distinguishing the two entities.

In the case of brain recurrence, the motion of protons is restricted due to increased cellular population, whereas in PIN proton motion is almost free due to necrosis. Thus tumour recurrence is associated with low apparent diffusion coefficient (ADC) values and PIN with higher values [59-71]. Although there is a difference in ADC values between these two entities, a significant overlap was recorded that relies on the intrinsic heterogeneity of GBM, with regions of high cellularity admixed with areas of necrosis, oedema, and microhaemorrhage. In addition, PIN has been found to consist not only of necrosis as expected, but also of foci of gliosis, fibrosis, vessels and cells such as macrophages that reduce proton motion and consequently reduce ADC values. In clinical practice however, recurrence and radiation necrosis are found to coexist in about 33% [59-71]. All of these factors limit

the efficiency of DWI technique. The recommended ADC cut-off value in discriminating recurrent neoplasm from radiation necrosis is $1.3 \times 10^{-3} \text{ mm}^2/\text{s}$. With the use of a higher b-value diffusion coefficient (b-value $4000 \text{ sec}/\text{mm}^2$) additional information can be gathered [59-71].

In the case of a recurring tumour, new vessel formation in PWI [59-71] produces an increase in rCBV values, in contrast to therapy-related changes (i.e. radiation necrosis, chemoradiation effects), in which ischaemic changes and cellular necrosis are associated with low rCBV values. The presence of small micro-haemorrhagic foci in case of reoccurrence reduces the mean rCBV values. The optimal cut-off thresholds vary significantly among studies. The reported rCBV cut-off ratios calculated for recurrence and radiation necrosis are over 2.6 and below 0.6 respectively [59-71]. It seems that lesions with higher rCBV values transform faster in higher degree gliomas in comparison to lesions with low rCBV values. Differences in the parameter results can result from tumour heterogeneity, variability in post-processing software, use of contrast preloading, selection of ROIs (size, number, location), and the evaluated DSC parameter (mean, maximum or histogram-derived percentile).

MRI spectroscopy [72-75] in brain tumour follow up assessment, may provide useful information regarding the peritumoural oedema, by discriminating oedema (normal metabolic ratios) from tumour infiltration (increased choline and decreased NAA). It can give information about treatment effectiveness and discrimination between recurrent or residual tumour high Cho/NAA ratios and post irradiation injury (low Cho/NAA ratio). Thus it can contribute to further treatment planning. The optimal cut-off choline/NAA ratio is still on debate, with a reasonable point may be the value of 2.2 [72-74]. Technical difficulties in spectroscopy arise from artefacts induced by haemorrhagic foci, bone, lipids and haemosiderin. Difficulties are also induced by lesions located in the periphery of the brain hemispheres and close to the calvaria. Another concern about spectroscopy is the lack of standardisation of imaging acquisition (e.g. 1.5T, 3T, short TE, long TE, single-voxel, multivoxel) among studies.

Bevacizumab, alone or in combination with other

agents, can reduce radiation necrosis by decreasing capillary leakage and the associated brain oedema.

SMART syndrome (migraine attacks after radiation therapy in a stroke-like pattern) is a rare syndrome seen in patients following cranial irradiation for central nervous system (CNS) malignancies [75-77]. Patients present with complex migraines and focal neurologic findings. It appears to be reversible, with possible age- and gender-related relations.

Radiation-induced vascular injury may produce a reversible vascular deregulation that leads in blood-brain barrier disruption and brain oedema, analogous to posterior reversible encephalopathy syndrome (PRES). The posterior cerebral hemispheres, primarily in the parieto-occipital region or cerebellum, are the typical locations. On MR imaging SMART syndrome typically shows gyriform cortical swelling with T2 hyperintensity (Fig. 7) and possible contrast enhancement [75-77]. In DWI some cases also show diffusion restriction. Other causes that cause similar imaging and should be ruled out are local tumour recurrence and leptomeningeal or ischaemic disease. MR imaging features improve or resolve spontaneously as does the clinical status, on follow-up imaging.

5b. Chemotherapy induced neurotoxicity

Chemotherapy induced toxicity depends on the toxic profile of the drug administered and the total dose [78-80]. The most common leukotoxic agent is methotrexate. Other commonly used agents are carmustine, cisplatin, cytarabine, fluorouracil and interleukin-2. The incidence of neurotoxicity is variable and depends upon the route of administration. It may occur in less than 10% of cases treated with intravenous methotrexate, but in up to 40% of cases treated with intrathecal methotrexate. It can manifest 1-2 weeks after initial administration. CNS toxicity is related with various structures, especially the white matter, producing toxic leukoencephalopathy. Clinical manifestation and imaging features are similar to post radiation leukoencephalopathy. MR imaging usually demonstrates frontoparietal white matter, non-enhancing T2 hyperintensity, sometimes depicts periventricular and deep white matter mainly diffuse or focal involvement. In the acute phase these lesions on DWI may restrict diffusion [81]. Other causes of toxic leukoencephalopathy

are imaged with analogous imaging characteristics. After discontinuation of chemotherapy the imaging findings are normalised [81].

A secondary form of hypophysitis is a well recognised chemotherapy-related side-effect of ipilimumab (immune-check-point inhibitor), the most established drug in the category [82-85]. Its incidence is estimated to be 4-9% of patients treated with this drug. Ipilimumab is a drug that blocks the T-cell inhibitor molecule CTLA-4 (Cytotoxic T Lymphocyte Antigen 4). Its function is the augmentation of the immune response. Many adverse autoimmune systemic reactions, such as colitis, dermatitis and arthritis may occur [82-86]. Importantly, many patients will go on to develop varying degrees of hypopituitarism, necessitating hormone replacement. Life-threatening hormonal imbalance can be caused, especially hypercortisolism. On imaging it is easy to diagnose, once one is familiar with the imaging appearance. MR imaging features are diffuse enlargement of the pituitary gland, often hypointense on T1-w imaging, with variable thickening/enlargement of the infundibulum. Follow-up imaging after drug cessation with concomitant introduction of steroids reveals complete resolution of abnormal findings and clinical symptoms.

5c. Pseudoprogression

Pseudoprogression (PP) is defined with the presence of new lesions or with an increase in contrast-enhancing previous lesions and perilesional oedema in patients with high-grade brain tumours treated with radiotherapy. PP occurs predominantly (in almost 60% of cases) within the first 3 months after completing treatment. The incidence of PP is around 36% for patients with high grade gliomas [46-50, 87-91] and 20% in patients with lower-grade gliomas. Clinical deterioration may accompany PP. It might be an indicator for better prognosis since it represents a more intense reaction to tumour response to the particular therapy. Therapy must be continued, discontinuation may produce true progression of the disease. Radiation and chemoradiation produce extensive necrotic areas to brain parenchyma, vascular thrombosis, fibrinoid necrosis and inflammation with a transient increase in permeability of the capillary bed of the examined area.

Conventional MRI demonstrates typical “Swiss cheese” or “soap bubble” pattern with increased contrast enhancement [88-91]. DWI is not specific for PP. PWI shows decreased rCBV values (**Fig. 6 II**), and its role is critical in PP diagnosis. On follow up examinations, decreased contrast enhancement and rCBV values (**Fig. 8 II**) are recorded.

Chemoradiation treatment-related PP [22-26] and radiation necrosis may show similar imaging findings. Chemoradiation is seen within the first 6 months from therapy initiation and usually subsides. Radiation necrosis usually appears one year following irradiation and produces more permanent changes. Advanced neuroimaging is crucial in differentiating between PP and progressive disease, especially PWI, with decreased values in the case of PP and increased values in the case of recurrence or progression.

Immunotherapy treatments focus on augmentation of the immune response and may produce similar imaging findings with PP (new appearing lesion or increase in the extension of the enhancing, already existing, lesion) within 6 months from the initiation of therapy, without clinical deterioration. At follow-up MR examination, 3 months later the lesion should disappear and this finding sets the diagnosis.

Transient seizure-related MR imaging changes produce similar imaging findings with PP and is known as peri-ictal pseudoproggression (PIPG). The development of a new cortical or leptomeningeal contrast-enhancing lesion in combination with frequent seizures should raise the suspicion of PIPG.

5d. Pseudoresponse

The human brain comprises over 100 million capillaries with a total length of 400 miles, a surface area of 20 m² and a median intercapillary distance of about 50 µm, making it the best perfused organ in the body. High grade gliomas create hypoxic conditions due to high metabolic demands and provoke the increased expression of vascular endothelial growth factor (VEGF) and angiogenesis with subsequent formation of abnormal blood vessels and dysfunction of blood brain tumour barrier.

Anti-angiogenic agents and bevacizumab (Anti-an-

giogenic agent) are monoclonic antibodies that block growth factor of VEGF and subsequent block and reduce cancer cell growth by reducing their blood supply. As a result, brain oedema and contrast medium enhancement of the area of interest are reduced.

Conventional and advanced MR imaging techniques (decreased ADC and rCBV values) demonstrate a feature of improvement, a condition known as pseudo-response (**Fig. 8**) [47-52]. In spectroscopy, increased levels of choline, lipids and lactic acid are seen. In follow-up imaging, the infiltrative nonenhancing tumoural component does not seem to be affected and eventually increases.

6. Conclusion

The evaluation of post-treatment response of brain gliomas is especially challenging in neuro-oncology. Surgery, radiation and chemotherapy can lead to the development of MRI features (contrast-enhanced and T2/FLAIR hyperintense lesions) that may mimic glioma progression. In many of new appearing lesions, tumour cells and post treatment injuries may coexist. Conventional MR imaging evaluates morphological brain tumour characteristics (size, necrosis, brain oedema, contrast enhancement) and physiological based MR neuroimaging functional characteristics such as cellularity (DWI), neovascularity (PWI) and metabolite consistency (spectroscopy). Brain lesions based on MR imaging are categorised according to RANO criteria. Even though classic and neurophysiological based MR imaging techniques can be extremely helpful in post treatment assessment of brain gliomas, the most reliable non-invasive method for the evaluation of the activity of the disease is the careful comparative examination of several follow up examinations. Attention should be focused on pseudophenomena such as pseudoproggression and pseudoresponse. **R**

Funding

This project did not receive any specific funding.

Conflict of interest

The authors declared no conflicts of interest.

REFERENCES

1. Omuro A, DeAngelis LM. Glioblastoma and other malignant gliomas. *JAMA* 2013; 310(17): 1842-1850.
2. Baker GJ, Yadav VN, Motsch S, et al. Mechanisms of glioma formation: Iterative perivascular glioma growth and invasion leads to tumor progression, VEGF-independent vascularization, and resistance to antiangiogenic therapy. *Neoplasia* 2014; 16(7): 543-561.
3. Weller M, Wick W, Aldape K, et al. Glioma. *Nat Rev Dis Prim* 2015; 1(1): 15017.
4. Ostrom QT, Gittleman H, Stetson L, et al. Epidemiology of gliomas. *Cancer Treat Res* 2015; 163: 1-14.
5. Placone AL, Quiñones-Hinojosa A, Searson PC. The role of astrocytes in the progression of brain cancer: complicating the picture of the tumor microenvironment. *Tumor Biol* 2016; 37(1): 61-69.
6. Alifieris C, Trafalis DT. Glioblastoma multiforme: Pathogenesis and treatment. *Pharmacol Ther* 2015; 152: 63-82.
7. Villanueva-Meyer JE, Mabray MC, Cha S. Current clinical brain tumor imaging. *Clin Neurosurg* 2017; 81(3): 397-415.
8. Mack SC, Hubert CG, Miller TE, et al. An epigenetic gateway to brain tumor cell identity. *Nat Neurosci* 2016; 19(1): 10-19.
9. David SC, Huda H, Helle BR, et al. Biomarkers in tumors of the central nervous system – a review. *APMIS* 2019; 127(5): 265-287.
10. Waitkus MS, Diplas BH, Yan H. Isocitrate dehydrogenase mutations in gliomas. *Neuro Oncol* 2016; 18(1): 16-26.
11. Bush NAO, Chang SM, Berger MS. Current and future strategies for treatment of glioma. *Neurosurg Rev* 2017; 40(1): 1-14.
12. Nam JY, de Groot JF. Treatment of glioblastoma. *J Oncol Pract* 2017; 13(10): 629-638.
13. Weller M, van den Bent M, Hopkins K, et al. EANO guideline for the diagnosis and treatment of anaplastic gliomas and glioblastoma. *Lancet Oncol* 2014; 15(9): e395-e403.
14. Jenkinson MD, Barone DG, Bryant A, et al. Intraoperative imaging technology to maximise extent of resection for glioma. *Cochrane Database Syst Rev* 2018; 1(1): CD012788.
15. Kuhnt D, Bauer MHA, Nimsky C. Brain shift compensation and neurosurgical image fusion using intraoperative MRI: Current status and future challenges. *Crit Rev Biomed Eng* 2012; 40(3): 175-185.
16. Zhang ZZ, Shields LBE, Sun DA, et al. The art of intraoperative glioma identification. *Front Oncol* 2015; 5: 175.
17. De Witt Hamer PC, Robles SG, et al. Impact of intraoperative stimulation brain mapping on glioma surgery outcome: A meta-analysis. *J Clin Oncol* 2012; 30(20): 2559-2265.
18. Riva M, Casarotti A, Comi A, et al. Brain and music: An intraoperative stimulation mapping study of a professional opera singer. *World Neurosurg* 2016; 93: 486.e13-18.
19. Hervey-Jumper SL, Berger MS. Maximizing safe resection of low- and high-grade glioma. *J Neurooncol* 2016; 130(2): 269-282.
20. Mert A, Kiesel B, Wöhrer A, et al. Introduction of a standardized multimodality image protocol for navigation-guided surgery of suspected low-grade gliomas. *Neurosurg Focus* 2015; 38(1): E4.
21. Taal W, Bromberg JEC, van den Bent MJ. Chemotherapy in CNS glioma. *Oncol* 2015; 4(3): 179-192.
22. Kreisl TN. Chemotherapy for malignant gliomas. *Semin Radiat Oncol* 2009; 19(3): 150-154.
23. Stupp R, Gander M, Leyvraz S, et al. Current and future developments in the use of temozolomide for the treatment of brain tumours. *Lancet Oncol* 2001; 2(9): 552-560.
24. Hart MG, Garside R, Rogers G, et al. Temozolomide for high grade glioma. *Cochrane Database Syst Rev* 2013; 2013(4): CD007415.
25. Khasraw M, Lassman AB. Advances in the treatment of malignant Gliomas. *Curr Oncol Rep* 2010; 12(1): 26-33.
26. Minniti G, Muni R, Caporello P, et al. Chemoradiation for glioblastoma. *Curr Drug Ther* 2010; 5(3): 157-163.
27. Sampson JH, Gunn MD, Fecci PE, et al. Brain immunology and immunotherapy in brain tumours. *Nat Rev Cancer* 2020; 20(1): 12-25.
28. Ranjan S, Quezado M, Garren N, et al. Clinical decision making in the era of immunotherapy for high

- grade-glioma: report of four cases. *BMC Cancer* 2018; 18(1): 239.
29. Huang RY, Neagu MR, Reardon DA, et al. Pitfalls in the neuroimaging of glioblastoma in the era of antiangiogenic and immuno/targeted therapy. Detecting illusive disease, defining response. *Front Neurol* 2015; 6: 33.
 30. Kosztyla R, Reinsberg SA, Moiseenko V, et al. Interhemispheric difference images from postoperative diffusion tensor imaging of gliomas. *Cureus* 2016; 8(10): e817.
 31. Sinclair AG, Scoffings DJ. Imaging of the post-operative cranium. *Radiographics* 2010; 30(2): 461-482.
 32. Warmuth-Metz M. Postoperative imaging after brain tumor resection. *Acta Neurochir* 2003; 88: 13-20.
 33. Macdonald DR, Cascino TL, Schold SC, et al. Response criteria for phase II studies of supratentorial malignant glioma. *J Clin Oncol* 1990; 8(7): 1277-1280.
 34. Law M, Oh S, Babb JS, et al. Low-grade gliomas: Dynamic susceptibility-weighted contrast-enhanced perfusion MR imaging-Prediction of patient clinical response. *Radiology* 2006; 238(2): 658-667.
 35. Chinot OL, Macdonald DR, Abrey LE, et al. Response assessment criteria for glioblastoma: Practical adaptation and implementation in clinical trials of antiangiogenic therapy. *Curr Neurol Neurosci Rep* 2013; 13(5): 347.
 36. Gerstner ER, Batchelor TT. Imaging and response criteria in gliomas. *Curr Opin Oncol* 2010; 22(6): 598-603.
 37. Lutz K, Radbruch A, Wiestler B, et al. Neuroradiological response criteria for high-grade gliomas. *Clin Neuroradiol* 2011; 21(4): 199-205.
 38. Lucas J, Zada G. Radiology: Criteria for determining response to treatment and recurrence of high-grade gliomas. *Neurosurg Clin N Am* 2012; 23(2): 269-276.
 39. Khan MN, Sharma AM, Pitz M, et al. High-grade glioma management and response assessment—recent advances and current challenges. *Curr Oncol* 2016; 23(4): e383-391.
 40. Leao DJ, Craig PG, Godoy LF, et al. Response assessment in neuro-oncology criteria for gliomas: Practical approach using conventional and advanced techniques. *AJNR Am J Neuroradiol* 2020; 41(1): 10-20.
 41. van Linde ME, Brahm CG, de Witt Hamer PC, et al. P08.71 Treatment outcome of patients with recurrent glioblastoma multiforme: a retrospective multicenter analysis. *J Neurooncol* 2017; 135(1): 183-192.
 42. Wen PY, Macdonald DR, Reardon DA, et al. Updated response assessment criteria for high-grade gliomas: Response assessment in neuro-oncology working group. *J Clin Oncol* 2010; 28(11): 1963-1972.
 43. Hesketh RL, Wang J, Wright AJ, et al. Magnetic resonance imaging is more sensitive than PET for detecting treatment-induced cell death-dependent changes in glycolysis. *Cancer Res* 2019; 79(14): 3557-3569.
 44. Sharma M, Juthani RG, Vogelbaum MA. Updated response assessment criteria for high-grade glioma: beyond the MacDonald criteria. *Chinese Clin Oncol* 2017; 6(4): 37.
 45. Wen PY, Chang SM, Van Den Bent MJ, et al. Response assessment in neuro-oncology clinical trials. *J Clin Oncol* 2017; 35(21): 2439-2449.
 46. Clarke JL, Chang S. Pseudoprogression and pseudoresponse: Challenges in brain tumor imaging. *Curr Neurol Neurosci Rep* 2009; 9(3): 241-246.
 47. Brandsma D, van den Bent MJ. Pseudoprogression and pseudoresponse in the treatment of gliomas. *Curr Opin Neurol* 2009; 22(6): 633-638.
 48. Hygino da Cruz LC Jr, Rodrigue I, Domingues RC, et al. Pseudoprogression and pseudoresponse: Imaging challenges in the assessment of posttreatment glioma. *AJNR Am J Neuroradiol* 2011; 32(11): 1978-1985.
 49. Thust SC, Van den Bent MJ, Smits MJ. Pseudoprogression of brain tumors. *Magn Reson Imaging* 2018; 48(3): 571-589.
 50. Rheims S, Ricard D, van den Bent M, et al. Peri-ictal pseudoprogression in patients with brain tumor. *Neuro Oncol* 2011; 13(7): 775-782.
 51. Holdhoff M, Ye X, Piotrowski AF, et al. The consistency of neuropathological diagnoses in patients undergoing surgery for suspected recurrence of glioblastoma. *J Neurooncol* 2019; 141(2): 347-354.
 52. Na A, Haghigi N, Drummond KJ. Cerebral radiation necrosis. *Asia Pac J Clin Oncol* 2014; 10(1): 11-21.
 53. Mehta S, Shah A, Jung H. Diagnosis and treatment options for sequelae following radiation treatment of brain tumors. *Clin Neurol Neurosurg* 2017; 163: 1-8.

54. Bisdas S, Naegel T, Ritz R, et al. Distinguishing recurrent high-grade gliomas from radiation injury. *Acad Radiol* 2011; 18(5): 575-583.
55. Shah R, Vattoth S, Jacob R, et al. Radiation necrosis in the brain: Imaging features and differentiation from tumor recurrence. *Radiographics* 2012; 32(5): 1343-1359.
56. Nael K, Bauer AH, Hormigo A, et al. Multiparametric MRI for differentiation of radiation necrosis from recurrent tumor in patients with treated glioblastoma. *AJR Am J Roentgenol* 2018; 210(1): 18-23.
57. Kumar AJ, Leeds NE, Fuller GN, et al. Malignant gliomas: MR imaging spectrum of radiation therapy- and chemotherapy-induced necrosis of the brain after treatment. *Radiology* 2000; 217(2): 377-384.
58. Lawrence YR, Li XA, el Naqa I, et al. Radiation dose-volume effects in the brain. *Int J Radiat Oncol* 2010; 76(3): S20-S27.
59. Upadhyay N, Waldman AD. Conventional MRI evaluation of gliomas. *Br J Radiol* 2011; 84(special_issue_2): S107-S111. doi:10.1259/bjr/65711810.
60. Rahmathulla G, Marko NF, Weil RJ. Cerebral radiation necrosis: A review of the pathobiology, diagnosis and management considerations. *J Clin Neurosci* 2013; 20(4): 485-502.
61. Zhou J, Tryggestad E, Wen Z, et al. Differentiation between glioma and radiation necrosis using molecular magnetic resonance imaging of endogenous proteins and peptides. *Nat Med* 2011; 17(1): 130-134.
62. Hyare H, Thust S, Rees J. Advanced MRI techniques in the monitoring of treatment of gliomas. *Curr Treat Options Neurol* 2017; 19(3): 11.
63. Mullins ME, Barest GD, Schaefer PW, et al. Radiation necrosis versus glioma recurrence: conventional MR imaging clues to diagnosis. *AJNR Am J Neuroradiol* 2005; 26(8): 1967-1972.
64. Hazle JD, Jackson EF, Schomer DF, et al. Dynamic imaging of intracranial lesions using fast spin-echo imaging: Differentiation of brain tumors and treatment effects. *J Magn Reson Imaging* 1997; 7(6): 1084-1093.
65. Svolos P, Kousi E, Kapsalaki E, et al. The role of diffusion and perfusion weighted imaging in the differential diagnosis of cerebral tumors: A review and future perspectives. *Cancer Imaging* 2014; 14(1): 20.
66. Hein PA, Eskey CJ, Dunn JF, et al. Diffusion-weighted imaging in the follow-up of treated high-grade gliomas: Tumor recurrence versus radiation injury. *AJNR Am J Neuroradiol* 2004; 25(2): 201-209.
67. Provenzale JM, Mukundan S, Barboriak DP. Diffusion-weighted and perfusion MR imaging for brain tumor characterization and assessment of treatment response. *Radiology* 2006; 239(3): 632-649.
68. Chao ST, Ahluwalia MS, Barnett GH, et al. Challenges with the diagnosis and treatment of cerebral radiation necrosis. *Int J Radiat Oncol* 2013; 87(3): 449-457.
69. Greene-Schloesser D, Robbins ME, Peiffer AM, et al. Radiation-induced brain injury: A review. *Front Oncol* 2012; 2: 73.
70. Asao C, Korogi Y, Kitajima M, et al. Diffusion-weighted imaging of radiation-induced brain injury for differentiation from tumor recurrence. *AJNR Am J Neuroradiol* 2005; 26(6): 1455-1460.
71. Zikou A, Sioka C, Alexiou GA, et al. Radiation necrosis, pseudoprogression, pseudoresponse, and tumor recurrence: Imaging challenges for the evaluation of treated gliomas. *Contrast Media Mol Imaging* 2018; 2018: 6828396.
72. Sundgren PC. MR spectroscopy in radiation injury. *AJNR Am J Neuroradiol* 2009; 30(8): 1469-1476.
73. Fink JR, Carr RB, Matsusue E, et al. Comparison of 3 Tesla proton MR spectroscopy, MR perfusion and MR diffusion for distinguishing glioma recurrence from posttreatment effects. *J Magn Reson Imaging* 2012; 35(1): 56-63.
74. Elmogy SA, Ezzat Mousa A, Elashry MS. MR spectroscopy in post-treatment follow up of brain tumors. *Egypt J Radiol Nucl Med* 2011; 42(3-4): 413-424.
75. de Oliveira Franco Á, Anzolin E, Schneider Medeiros M, et al. SMART syndrome identification and successful treatment. *Case Rep Neurol* 2021; 13: 40-45.
76. Kerklaan JP, Lycklama á Nijeholt GJ, Wiggeraad RG, et al. SMART syndrome: a late reversible complication after radiation therapy for brain tumours. *J Neurol* 2011; 258(6): 1098-1104.
77. Jaraba S, Puig O, Miró J, et al. Refractory status epilepticus due to SMART syndrome. *Epilepsy Behav* 2015; 49: 189-192.
78. Vos MJ, Uitdehaag BMJ, Barkhof F, et al. Interob-

- server variability in the radiological assessment of response to chemotherapy in glioma. *Neurology* 2003; 60(5): 826-830.
79. Kumar Y, Drumsta D, Mangla M, et al. Toxins in brain! magnetic resonance (Mr) imaging of toxic leukoencephalopathy – a pictorial essay. *Pol J Radiol* 2017; 82: 311-319.
 80. Moore-Maxwell CA, Datto MB, Hulette CM. Chemotherapy-induced toxic leukoencephalopathy causes a wide range of symptoms: a series of four autopsies. *Mod Pathol* 2004; 17(2): 241-247.
 81. McKinney AM, Kieffer SA, Paylor RT, et al. Acute toxic leukoencephalopathy: Potential for reversibility clinically and on MRI Wwth diffusion-weighted and FLAIR imaging. *AJR Am J Roentgenol* 2009; 193(1): 192-206.
 82. Salkade PR, Lim TA. Methotrexate-induced acute toxic leukoencephalopathy. *J Cancer Res Ther* 2012; 8(2): 292-296.
 83. Bot I, Blank CU, Boogerd W, et al. Neurological immune-related adverse events of ipilimumab. *Pract Neurol* 2013; 13(4): 278-280.
 84. Iwama S, De Remigis A, Callahan MK, et al. Pituitary expression of CTLA-4 mediates hypophysitis secondary to Administration of CTLA-4 blocking antibody. *Sci Transl Med* 2014; 6(230): 230ra45.
 85. Albarel F, Gaudy C, Castinetti F, et al. Long-term follow-up of ipilimumab-induced hypophysitis, a common adverse event of the anti-CTLA-4 antibody in melanoma. *Eur J Endocrinol* 2015; 172(2): 195-204.
 86. Joshi MN, Whitelaw BC, Palomar MTP, et al. Immune checkpoint inhibitor-related hypophysitis and endocrine dysfunction: clinical review. *Clin Endocrinol (Oxf)* 2016; 85(3): 331-339.
 87. Fink J, Born D, Chamberlain MC. Pseudoprogression: relevance with respect to treatment of high-grade gliomas. *Curr Treat Options Oncol* 2011; 12(3): 240-252.
 88. González-Suárez I, Aguilar-Amat MJ, Trigueros M, et al. Leukoencephalopathy due to oral methotrexate. *Cerebellum* 2014; 13(1): 178-183.
 89. Ismail M, Hill V, Statsevych V, et al. Shape features of the lesion habitat to differentiate brain tumor progression from pseudoprogression on routine multiparametric MRI: A multisite study. *AJNR Am J Neuroradiol* 2018; 39(12): 2187-2193.
 90. Matsuo M, Tanaka H, Yamaguchi T, et al. Pseudoprogression of glioblastoma multiforme after chemoradiation therapy: Diagnosis by 11C-methionine Positron Emission Tomography (PET). *Int J Radiat Oncol* 2016; 96(2): E102.
 91. Galldiks N, Kocher M, Langen KJ. Pseudoprogression after glioma therapy: an update. *Expert Rev Neurother* 2017; 17(11): 1109-1115.



READY - MADE
CITATION

Voultsinou D, Gerukis T. Post-treatment Magnetic Resonance Imaging assessment of brain gliomas. *Hell J Radiol* 2021; 6(1): 56-71.